Al-Kitab Journal for Pure Sciences (2026); 10(2):24-40.
https://doi.org/10.32441/kjps.10.2.p3

Al-Kitab Journal for Pure Sciences
ISSN: 2617-1260 (print), 2617-8141(online)

https://isnra.net/index.php/kjps

Computational Study of the Properties of the Medicinal Compound Tromantadine

Zeena R. Katoof[1], Athra G. Sager[2], Jawad Kadhim Abaies[3]

[1,2,3]Department of Chemistry, College of Science, University of Wasit, Wasit, Iraq.

Corresponding Author: asaker@uowasit.edu.iq

Citation: *Zeena R. Katoof[1], Athra G. Sager[2], Jawad Kadhim Abaies[3]*. **Computational Study of the Properties of the Medicinal Compound Tromantadine.**
Al-Kitab J. Pure Sci. [Internet]. 2025 Aug. 17 ;10(2):24-40
DOI.
https://isnra.net/index.php/kjps/article/view/2026.
https://doi.org/10.32441/kjps.10.2.p3.

Keywords: DFT, Gaussin, Herpes,Virus, Tromantadine.

Article History

Received	19 Jun.	2025
Accepted	17 Aug.	2025
Available online	01 Nov.	2026

©20--. THIS IS AN OPEN-ACCESS ARTICLE UNDER THE CC BY LICENSE
http://creativecommons.org/licenses/by/4.0/

Abstract:

Tromantadine is a medicine commonly prescribed for treating the herpes simplex virus. In this work, computational methods, including density functional theory (DFT) and molecular docking simulations, were utilized to investigate the antiviral potential activity of Tromantadine. The structural optimization and quantum chemical analysis were performed via Density Functional Theory (DFT) at the B3LYP/6-311^{++}G (d,p) level using GAUSSIAN 09, while molecular docking against Herpes Simplex Virus (HSV) proteins-DNA polymerase (PDB ID: 8OJA) and glycoprotein (PDB ID: 3SKU) was conducted using MOE 2019. Electronic descriptors, energy gap, Mulliken charges, and Fukui functions were evaluated to identify the key reactive sites of the targeted proteins. The molecular docking results revealed a favorable binding affinity of Tromantadine with both viral targets, suggesting its potential effectiveness as an inhibitor for HSV replication and entry. These findings warrant further in vitro and in vivo experimental validation.

Keywords: DFT, Gaussin, Herpes,Virus, Tromantadine.

دراسة حسابية لخصائص المركب الطبي ترومانتادين

زينه رزاق كطوف[1]، عذراء كطامي صكر[2]، جواد كاظم عبيس[3]

[1,2,3]قسم علوم الكيمياء ، كلية العلوم، جامعة واسط، واسط، العراق

الايميل الرسمي: zeenarazaq22@gmail.com , asaker@uowasit.edu.iq, jabaies@uowasit.edu.iq

الخلاصة:

يُوصف دواء الترومانتادين عادةً لعلاج فيروس الهربس البسيط. في هذا البحث، استُخدمت أساليب حسابية، بما في ذلك نظرية الكثافة الوظيفية (*DFT*) ومحاكاة الالتحام الجزيئي، لدراسة النشاط المحتمل للترومانتادين كمضاد للفيروسات. أُجري التحسين الهيكلي والتحليل الكيميائي الكمي باستخدام نظرية الكثافة الوظيفية (*DFT*) عند مستوى *B3LYP/6-311^{++}G (d,p)* باستخدام *GAUSSIAN 09*، بينما أُجرِيَ الالتحام الجزيئي ضد بروتينات فيروس الهربس البسيط (*HSV*) - بوليميراز الحمض النووي (معرف قاعدة بيانات البروتين: *OJA٨*) والبروتين السكري (معرف قاعدة بيانات البروتين: *SKU٣*) باستخدام *MOE 2019*، قُيِّمت الواصفات الإلكترونية، وفجوة طاقة، وشحنات موليكن، ووظائف فوكوي لتحديد المواقع التفاعلية الرئيسة للبروتينات المستهدفة، وأظهرت نتائج الالتحام الجزيئي تقاربًا إيجابيًا لترابط ترومانتادين مع كلا الهدفين الفيروسيين، مما يشير إلى فعاليته المحتملة كمثبط لتكاثر فيروس الهربس البسيط واختراقه، وتستدعي هذه النتائج مزيدًا من التحقق التجريبي في المختبر وفي الجسم الحي.

الكلمات المفتاحية: *DFT* , برنامج الغاوسين ، فيروس الهربس ، ترومانتادين

1. Introduction:

Antiviral medicines, Tromantadine, was utilized for therapy of herpes simplex virus. Commercially, this medicine is known as Viru-Merz and Viru-Merz Serol. Tromantadine's IUPAC name is N-(1-adamantyl)-2-[1] (dimethylamino)ethoxy]acetamide see Figure 1. Tromantadine is obtainable in a local gel, and its performance is very close to acyclovir action [2,3]. Similar to rimantadine, and amantadine, Tromantadine is an adamantine derivative. It was established that the early and late processes in the virus DNA duplication cycle are inhibited by Tromantadine[4]. This medicine targets the glycoproteins of the host cells through variations, resulting in obstruction of the virus absorption. It inhibits the penetration of the virus. As Tromantadine obstructs the uncoating of the virions, virus penetration is inhibited [5-7]. As a category of antimicrobials, antivirals are a broad range of medicines. On the basis of monoclonal antibodies, this category also comprises antibiotics, antifungals and antiviral drugs. To some extent, the majority of these antivirals drugs are regarded as safe medications, so they are prescribed for treating diversity of infections [8]. Nowadays, the computational techniques are considered dependable theoretical methods and promising

approaches in medical industries to discover new drugs with potential activities and applications [9-11].

This study aims to examine the antiviral efficacy of Tromantadine against Herpes Simplex Virus (HSV) using computational techniques, including density functional theory (DFT) analysis and molecular docking, and assess its binding affinity and identify its potential inhibitory effects.

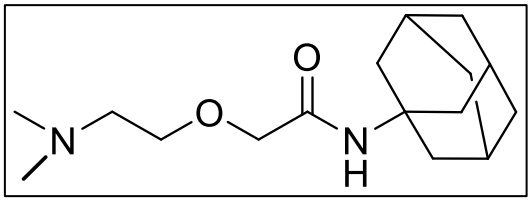


Figure 1. Structure of Tromantadine

2. Materials and Methods :

2.1 Computational methods.

The computational study was carried out using the GAUSSIAN 09W software package [12,13]. All calculations were accomplished utilizing a personal computer with an Intel Core i7 processor (HP). Density Functional Theory (DFT) calculations were performed using the B3LYP functional and the 6-311^{++}G basis set [14,15]. The antiviral medicine, Tromantadine, was chosen as the subject of the analysis. The docking simulations were performed using two protein targets: DNA polymerase (8OJA) and Glycoprotein (3SKU), which were obtained from web the Protein Data Bank.

2.2 Excretion, and toxicity (ADMET)

Several drugs failed in clinical trials and further development stages due to unpleasant pharmacological properties and other unfavourable results. In this study, Tromantadine was investigated using the Swiss ADME website. In silico toxicity testing was performed using the website ProTox-II, which is provided a projected oral toxicity, cytotoxicity, mutagenicity, carcinogenicity, hepatotoxicity, and immune toxicity values for the compound.

3. Results and Discussion:

3.1 Energy band gaps

Computational study process started with finding out the optimized molecular structure of the molecule under study (Figure 2). The optimized molecular structure of tromantadine was ascertained utilizing DFT(6-311^{++}G basis set) at a vacuum. In this step, numbering of the atoms and the molecule orientation were established. Table 1 below illustrates the definite

geometrical parameters of the medicine molecule. The length of the bond between C(17)-C(19) in the ring is 1.556 Å and it is1.427 Å for N(4)-C(11) in the side. Nevertheless, the bond length of C(6)-C(7)in the chain = 1.528 Å. Furthermore, the C(17)-C(18) bond length in the ring = 1.540 Å, and is 1.045 Å of the N(4)-H(23) out of the chain, while for O(5)-C(6) = 1.414 Å. The bond length of C(1)-O(3) in C=O and C(14)-H(38) in N-H =1.225, and 1.427. Å, respectively. which it was confirmed that the tromantadine possesses a good activity as the atom angles in its arrangement were typical.

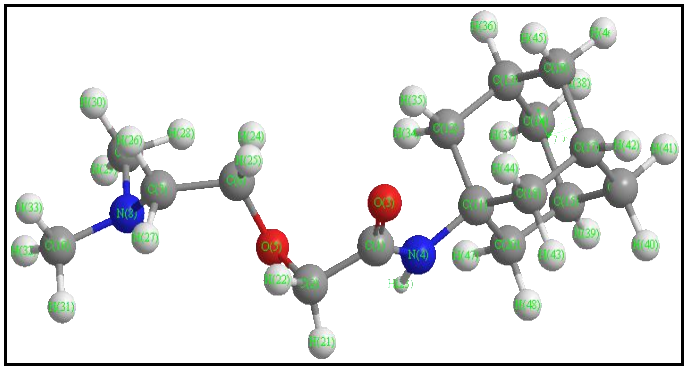


Figure 2. Tromantadine structure with symbols of Atoms

Table 1. Geometrical parameters of Tromantadine medicine

Atoms	*bond length* (Å)	*Atoms*	*Bond angles(Å)*	*Atoms*	*Dihedral(Å)*
C(20)-H(48)	1.104	H(42)-C(17)-C(19)	109.39	C(16)-C(17) C(19)-C(13)	55.576
C(20)-H(47)	1.092	H(42)-C(17)-C(18)	109.39	C(16)-C(17)-C(19)-H(45)	172.685
C(19)-H(46)	1.103	H(42)-C(17)-C(16)	109.39	C(16)-C(17)-C(19)-H(46)	-66. 053
C(19)-H(45)	1.079	C(19)-C(17)-C(18)	109.51	C(18)-C(17)-C(19)-C(13)	-65. 791
C(18)-H(44)	1.077	C(19)-C(17)-C(16)	109.51	C(18)-C(17)-C(19)-H(45)	51.318
C(18)-H(43)	1.074	C(18)-C(17)-C(16)	109.51	C(18)-C(17)-C(19)-H(46)	172.580
C(17)-H(42)	1.128	H(41)-C(16)-H(40)	109.4	H(42)-C(17)-C(19)-C(13)	172.178
C(17)-C(19)	1.558	H(41)-C(16)-C(17)	109.410	H(42)-C(17)-C(19)-H(45)	-70. 713
C(17)-C(18)	1.525	H(41)-C(16)-C(15)	109.410	H(42)-C(17)-C(19)-H(46)	50.549
C(16)-H(41)	1.097	H(40)-C(16)-C(17)	109.410	C(16)-C(17)-C(18)-C(11)	-58. 130
C(16)-H(40)	1.077	H(40)-C(16)-C(15)	109.410	C(16)-C(17)-C(18)-H(43)	64.822
C(16)-C(17)	1.563	C(17)-C(16)-C(15)	109.500	C(16)-C(17)-C(18)-H(44)	-17 6.77
C(15)-H(39)	1.129	H(39)-C(15)-C(20)	109.390	C(19)-C(17)-C(18)-C(11)	61.447
C(15)-C(20)	1.595	H(39)-C(15)-C(16)	109.390	C(19)-C(17)-C(18)-H(43)	-17 5.60
C(15)-C(16)	1.514	H(39)-C(15)-C(14)	109.390	C(19)-C(17)-C(18)-H(44)	-57. 201
C(14)-H(38)	1.146	C(20)-C(15)-C(16)	109.510	H(42)-C(17)-C(18)-C(11)	-17 7.80
C(14)-H(37)	1.154	C(20)-C(15)-C(14)	109.510	H(42)-C(17)-C(18)-H(43)	-54.8
C(14)-C(15)	1.552	C(16)-C(15)-C(14)	109.510	H(42)-C(17)-C(18)-H(44)	63.545

C(13)-H(36)	1.123	H(46)-C(19)-H(45)	109.400	C(15)-C(16)-C(17)-C(18)	62.329
C(13)-C(19)	1.498	H(46)-C(19)-C(17)	109.410	C(15)-C(16)-C(17)-C(19)	-5 6.38
C(13)-C(14)	1.538	H(46)-C(19)-C(13)	109.410	C(15)-C(16)-C(17)-H(42)	-17 4.98
C(12)-H(35)	1.121	H(45)-C(19)-C(17)	109.410	H(40)-C(16)-C(17)-C(18)	-54. 780
C(12)-H(34)	1.120	H(45)-C(19)-C(13)	109.410	H(40)-C(16)-C(17)-C(19)	-17 3.49
C(12)-C(13)	1.531	C(17)-C(19)-C(13)	109.500	H(40)-C(16)-C(17)-H(42)	67.91
C(11)-C(20)	1.576	H(38)-C(14)-H(37)	109.400	H(41)-C(16)-C(17)-C(18)	-17 5.92
C(11)-C(18)	1.616	H(38)-C(14)-C(15)	109.410	H(41)-C(16)-C(17)-C(19)	65.356
C(11)-C(12)	1.613	H(38)-C(14)-C(13)	109.410	H(41)-C(16)-C(17)-H(42)	-53. 235
C(10)-H(33)	1.080	H(37)-C(14)-C(15)	109.410	C(14)-C(15)-C(20)-C(11)	-59. 743
C(10)-H(32)	1.097	H(37)-C(14)-C(13)	109.410	C(14)-C(15)-C(20)-H(47)	65.338
C(10)-H(31)	1.098	C(15)-C(14) C(13)	109.500	C(14)-C(15)-C(20)-H(48)	-17 9.57
C(9)-H(30)	1.069	H(36)-C(13) -C(19)	109.390	C(16)-C(15)-C(20)-C(11)	59.882
C(9)-H(29)	1.079	H(36)-C(13)-C(14)	109.390	C(16)-C(15)-C(20)-H(47)	-17 5.03
C(9)-H(28)	1.068	H(36)-C(13)-C(12)	109.390	C(16)-C(15)-C(20)-H(48)	-59. 949
N(8)-C(10)	1.467	C(19)-C(13)-C(14)	109.510	H(39)-C(15)-C(20)-C(11)	-17 8.18
N(8)-C(9)	1.502	C(19)-C(13)-C(12)	109.510	H(39)-C(15)-C(20)-H(47)	-53. 103
C(7)-H(27)	1.063	C(14)-C(13)-C(12)	109.510	H(39)-C(15)-C(20)-H(48)	61.985
C(7)-H(26)	1.114	H(48)-C(20)-H(47)	109.400	C(14)-C(15)-C(16)-C(17)	60.658
C(7)-N(8)	1.514	H(48)-C(20)-C(15)	109.410	C(14)-C(15)-C(16)-H(40)	-17 9.70
C(6)-H(25)	1.145	H(48)-C(20)-C(11)	109.410	C(14)-C(15)-C(16)-H(41)	-57. 806
C(6)-H(24)	1.081	H(47)-C(20)-C(15)	109.410	C(20)-C(15)-C(16)-C(17)	-60. 289
C(6)-C(7)	1.527	H(47)-C(20)-C(11)	109.410	C(20)-C(15)-C(16)-H(40)	59. 350
O(5)-C(6)	1.427	C(15)-C(20)-C(11)	109.500	C(20)-C(15)-C(16)-H(41)	-17 8.75
N(4)-H(23)	1.007	H(44)-C(18)-H(43)	109.400	H(39)-C(15)-C(16)-C(17)	179.886

3.2 Study of Mulliken charge and correlation with quantum chemical distribution of Tromantadine

To decide the major reactive spots in the arrangement and to differentiate between types of reactions, Frontier Molecular Orbitals (FMOs) have been employed. The energy of the lowest unoccupied molecular orbital (LUMO) and the highest occupied molecular orbital (HOMO), and their energy difference (ΔE) were utilized to evaluate the molecule reactivity. For Tromantadine medicine, the level B3LYP/6-31^{++}G (d, p) was utilized to calculate HOMO and LOMO energies as shown in Figure 3. The minimal electronic energy that required for the electron transition n–π* is represented by the (HOMO – LUMO) energy difference gab. The HOMO energy average at 77th was calculated at -0.23179 eV and LOMO slightest energy at

78th was calculated at -0.01571 eV for the molecule under test, Tromantadine. Upon the optimization of the current molecule arrangement, the (HOMO – LUMO) energy band gab was calculated from MOs and found = 2.0324638 eV. Although this value indicates that the energy band gap of Tromantadine is high, the stability of its structure is significant. Parameters for Tromantadine, including chemical hardness, electronegativity, electronic chemical potential, and electro-philicity index were measured utilizing DFT and the results were listed in Table 2. The following are parameters for Tromantadine molecule [16-18]:

- The HOMO energy (EHOMO).
- The LUMO energy (ELUMO).
- The energy gap between EHOMO and ELUMO (ΔE=HOMO-LUMO) .
- Electronegativity(χ).
- Dipole moment (μ).
- Electron affinity(A).
- Ionization energy (IP).
- Softness(s),global hardness(η).
- Global electrophilicity (ω).

Based on molecular gas-phase of Tromantadine molecule, the distribution of density for LUMO and HOMO is displayed in Figure 3. In the medicine structure, the highes electronic density is specified by the red color area, which represented by C6, C7, and N8 atoms, wherese, the lesser electron density is specified by the green color site. Due to the double bond and aromatic ring moities of the inhibitor structure, it possesses a significant electronic density. It can be noticed that, the greatest electronic density focused over atom N8 atom in $N(CH_3)_2$ segment of Tromantadine structure.

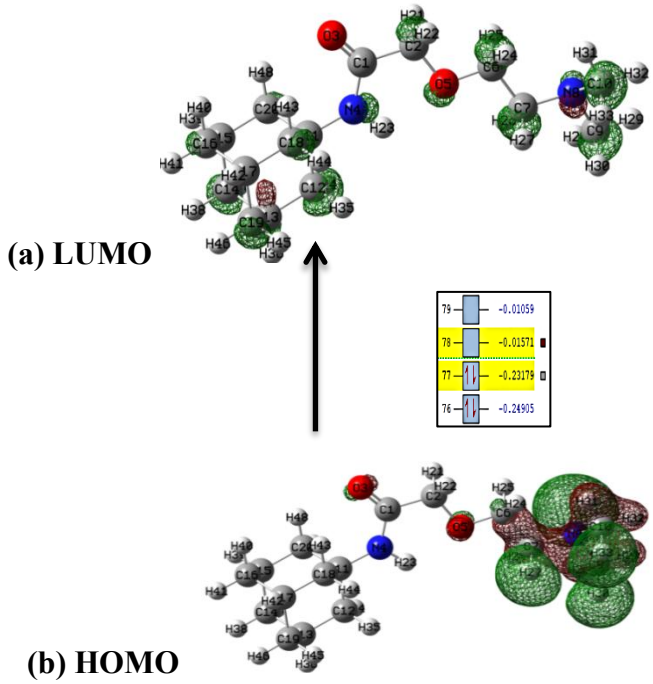


Figure 3. Frontier surfaces for Tromantadine(a)LUMO and (b) HOMO

Fukui functions calculation determine the active atoms in the molecule. This calculation is related to the electronic density variations. To calculate of Fukui functions, Equations (1,2 and 3) f+(r) , f-(r) and f0(r) were employed [19-21]:

$$f^{+} = [q(N+1) - q(N)] \quad \ldots \quad (1) \text{ nucleophilic species}$$

$$f^{-} = [q(N) - q(N-1)] \quad \ldots \quad (2) \text{ electrophilic species}$$

$$f^{0} = [q(N+1) - q(N-1)]/2 \quad \ldots \quad (3) \text{ free radicals species}$$

Where: the charge located on atoms in neutral classes is represented by q(N), the atomic positive charges in cationic species are implied by q(N+1), and the atomic anionic charges are signified by q (N-1) [22]. Table. 3 illustrates the descriptor values that were calculated by Mulliken charges over the atom of the molecule structure. As shown in Figure 3, the distribution of the charges on the atom was evaluated via Mulliken equation. The calculated Fukui functions provide additional information about the molecule reactive sites. Carbon atoms (9C and 10C) have the highest dual reactivity for both nucleophilic (f^{+1} = 0.173, 0.174) and electrophilic (f^{-1} = 0.236, 0.159) attacks, making them the most chemically active centres. Remarkably, Carbon atom (13C) showed an exceptionally high electrophilic reactivity (f^{-} = 1.569), indicating a potential site for strong electron donation. Conversely, other atoms such as 5O and 6C showed minimal or even negative Fukui values, suggesting low or negligible participation in chemical reactions. The carbon atom (13C) exhibited a high electrophilic reactivity (f^{1}=1.569), suggesting a potential site for strong electron donation. In contrast,

atoms such as 5O and 6C had minimum or even negative Fukui values, indicating a little or no participation in the chemical reactions. Furthermore, the carbon atoms (13C and C17) showed an exceptionally high free radical reactivity (f^0=0.778876,0.374119). The atoms (8N and 9C) have the greatest exposure to electrophilic species reactions. These calculations were performed to investigate the electronic structure of Tromantadine and assess its bioactivity.

The Mulliken charge analysis revealed a significant variations in electronic distribution throughout the molecule, which denotes concentrated areas with high electron density. Thus, these sites are expected to serve as nucleophilic centres, enabling of generating hydrogen bonds and coordinating interactions with electrophilic sites on viral proteins. Conversely, electron-deficient regions are more likely to interact with electron-rich (nucleophilic) groups found in viral components such as glycoproteins and nucleic acids. This intramolecular polarity distribution identifies possible active areas through which Teromatin can interact with viral targets. The HOMO energy was computed at -6.307 eV and the LUMO energy at -4.275 eV, yielding an energy gap(ΔE)of 2.03 eV (Table 2). This moderate band gap indicates an appropriate chemical reactivity for biological interactions. The chemical hardness (η = 2.94eV) and electronegativity (χ =3.37eV) values show the molecule resistance to charge deformation and its ability to attract electrons. The softness (S=0.34eV) indicates the flexibility of the electron cloud. Tromantadine has a high electrophilicity index (ω=1.93 eV), indicating its ability to accept electrons and interact with electron-rich active sites in the virus. The dipole moment (3.67 Debye) emphasises the molecule polarity, increasing its water solubility and enabling contact with polar viral surfaces. Collectively, these electronic and structural properties demonstrate that Tromantadine is well-suited to interact with HSVtargets via hydrogen bonding and electrostatic interactions with viral proteins or genetic material. Cosequenyely, it potentially inhibiting the viral replication cycle Figure 4.

Table 2. Quantum chemical parameters for Tromantadine in vacuum medium

Parameter	Value	Parameter	Value
EHOMO (a.u)	-6.307469 (eV)	ELUMO (a.u)	-4.2750052 (eV)
IE= -EHOMO	6.037469(eV)	ΔE =HOMO - LOMO	-2.0324638(eV)
EA= -ELUMO	4.2750052(eV)	S =[1/2η]	0.340134(eV)
CP	-3.36749(eV)	$\omega = \left(\frac{\mu 2}{2\eta}\right)$	1.928574(eV)
Nmax	1.14540 (eV)	X =[(IP+EA)/2]	3.367485(eV)
So	0.17006 (eV)	Ŋ=[ELOMO-EHOMO]/2	2.939984(eV)
(μ)	3.66722*(Debye)*	EA	0.427501(eV)

Table 3. Mulliken atomic charges distribution.

Atoms	*n*	*n+1*	*n-1*	f^{+1}	f^{-1}	f^{0}
1C	0.38	0.415501	0.287376	0.035501	0.092624	0.064063
2C	0.014871	0.094837	-0.05378	0.079966	0.068653	0.07431
3O	-0.38577	-0.24308	-0.40192	**0.142695**	0.016153	0.079424
4N	0.670015	0.739273	1.022085	0.069258	-0.35207	-0.14141
5O	-0.30051	-0.30028	-0.2966	0.000231	-0.00391	-0.00184
6C	0.052123	0.049837	0.216372	-0.00229	-0.16425	-0.08327
7C	-0.10067	0.0401	0.007068	0.14077	-0.10774	0.016516
8N	0.001455	0.024892	-0.17317	0.023437	**0.174623**	0.09903
9C	0.149082	0.321834	-0.08691	**0.172752**	**0.235991**	0.204372
10C	0.078181	0.251909	-0.08039	**0.173728**	0.158571	0.16615
11C	-1.84057	-2.10509	-1.39697	-0.26452	-0.4436	-0.35406
12C	-0.14539	-0.06631	-0.11369	0.079079	-0.0317	0.023688
13C	0.476269	0.464657	-1.09309	-0.01161	**1.569363**	**0.778876**
14C	-0.32702	-0.26338	0.343588	0.063645	-0.67061	-0.30348
15C	0.4619	0.432179	-0.24903	-0.02972	0.710933	0.340606
16C	-0.21634	-0.1473	0.259176	0.069044	-0.47552	-0.20324
17C	0.453838	0.420594	-0.32764	-0.03324	0.781481	**0.374119**
18C	0.461948	0.580397	0.425512	0.118449	0.036436	0.077443
19C	-0.32661	-0.26387	0.337688	0.062742	-0.6643	-0.30078
20C	0.440801	0.553289	0.374338	0.112488	0.066463	0.089476

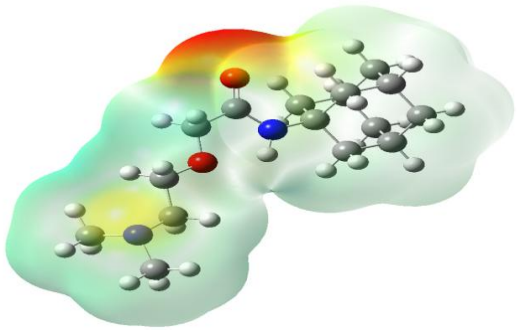


Figure 4. Electrostatic Potential Map

3.3 Molucular docking analysis

Herpes simplex virus (HSV-1), a double-stranded DNA virus, replicates with seven essential proteins encoded in its genome. Among these protiens, the UL30 DNA polymerase, in conjunction with the UL42 processivity factor, coordinates leading and lagging strand replication of the 152 kb viral genome 23]. Docking of Tromantidine (T) was performed to investigate the compound stabilising interactions within the protein pockets of the chosen

target. This research was carried out utilising MOE-2019 software. DNA polymerase (PDBID:8OJA(A)) and Glycoprotein (PDBID:3SKU(D)) were downloaded from an internet data bank server at https://www.rcsb.org/pdb and stored in Pdb format [24]. Tromantadine three-dimensional structure was created using the Gaussian 09W software. This was done by standard protocols for ligand and protein preparation, which include energy minimization and the active site identification (see Table 4). The docking results demonstrated a favourable interaction between Tromantadine and the target Glycoprotein (see Table 5 and Figure 5) . While they did not show any interaction between Tromantadines and the DNA polymerase. In the case of 3SKU, Tromantadine exhibited a modrate binding affinity, forming one key hydrogen bond (H-acceptor) within the active site pocket, particularly with the residue LYS190(A). The binding energy was estimated to be (-4.741 kcal/mol), indicating a stable complex formation(see Figure 5 . Similarly, the docking of Acyclovi (conterol) with DNA polymerase (8OJA) revealed notable interactions through hydrogen bonding. Thymotadine was observed to engage with crucial surface residues, possibly interfering with the virus-host cell attachment mechanism. The calculated binding energy for this complex was (-5.248 kcal/mol). These results suggest that Tromantadine could potentially inhibit HSV replication through once targeting mechanism through preventing viral entry through glycoprotein interference. While the acyclovir results suggest that acyclovir could potentially inhibit HSV replication through dual targeting mechanisms. Firstly, obstructing DNA synthesis via polymerase inhibition, and secondly by preventing viral entry through glycoprotein interference(see Table 5 and Figure 5). The docking outcomes provide a theoretical basis for further in vitro and in vivo antiviral evaluations of Tromantadine as a favourable therapeutic candidate against HSV infection.

Table 4. Binding site residues as input for receptor grid generation throughout docking

Receptor	PLB	Hyd	Side	Residues
8OJA	2.95	24	41	1:(HIS148 VAL311 PHE313 GLY314 TRP315 ILE352 GLY355 MET356 SER357 ASP358 LEU359 HIS595 LEU596 SER59ALA600 ARG603 LEU802 LYS805 GLN806)
3SKU	5.00	56	90	1:(ASP368 ILE369 GLU370 CYS371 LYS372 ALA373 GLU378 LEU379 ALA380 PRO382 GLU426 TYR465 ASN466 PHE470 ASP471 LYS539 LEU540 ASN541 LYS552 LYS553 ASP554 LEU555 SER556 TYR557 ARG558 ILE560 PRO561 ILE574 GLU576 TYR577 CYS578 GLN580 ASP581

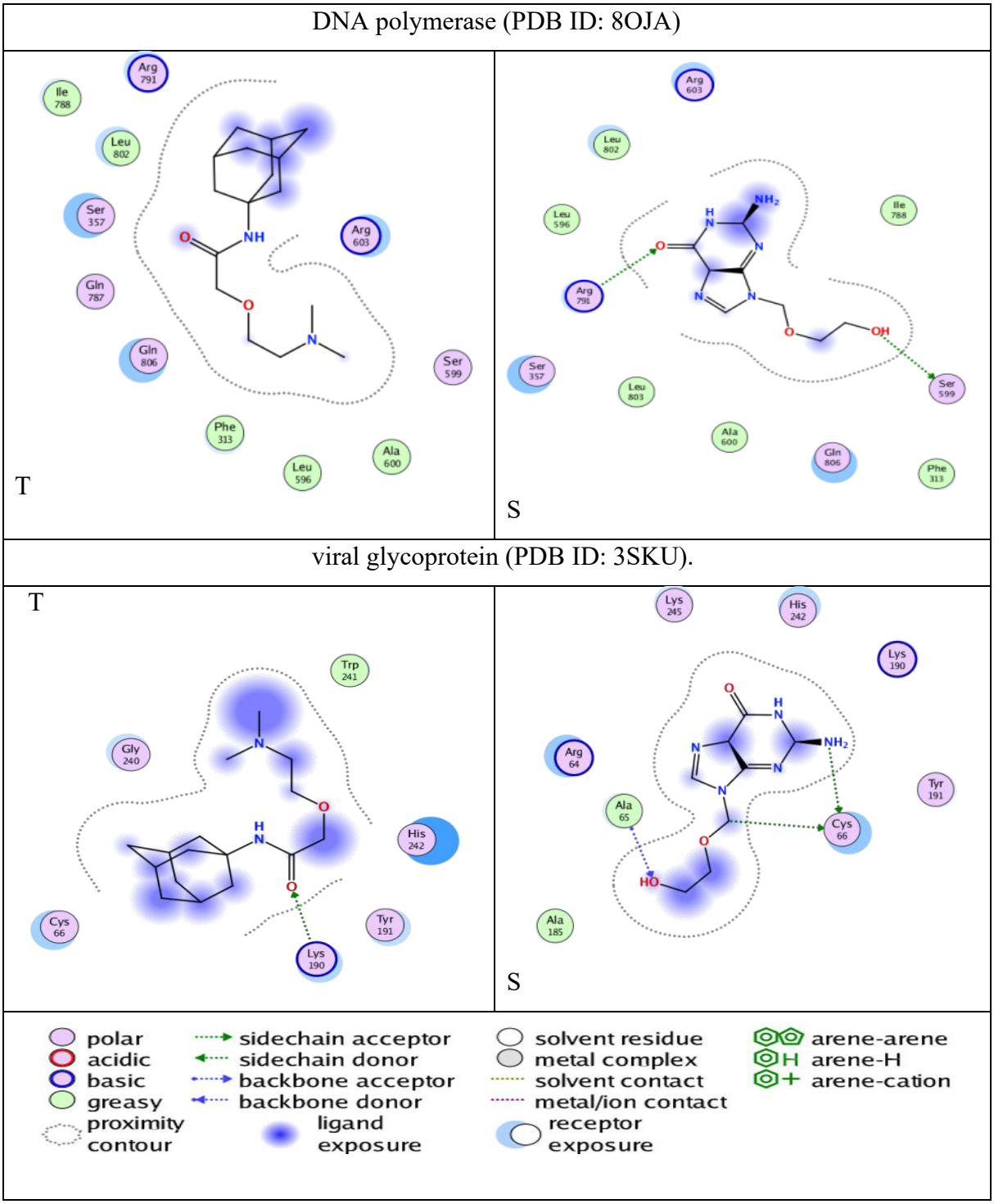


Figure 5. 2D Binding site interaction of Tromantadine (T) and Acyclovi (S) a with DNA polymerase (PDB ID: 8OJA) and the viral glycoprotein (PDB ID: 3SKU).

Table 5 . Docking findings of compounds (Tromantadine and Acyclovi)with(8OJA &3SKU) in site (1)

Code Drug	Receptor	S-score (kcal/ mol)	RMSD (Å)	Bonding between atoms of compounds and residues of the active site 1 in 3OG7					
				Atom of compound	Atom of receptor	Involved receptor residues	Interaction bond	Distance (Å)	E(Kcal /mol)
T	8OJA	-5.6217	2.358	-	-	-	-	-	-
Acy	8OJA	-5.248	1.501	O 16 O8	OG NH2	SER599(A) AGR791(A)	H-donor H-acceptor	3.03 3.4	-0.5 -0.8
T	3SKU	-4.741	2.158	O12	NZ	LYS190(A)	H-acceptor	2.59	-0.9
Acy	3SKU	-4.491	1.750	N7 C 12 O 16	SG SG N	CYS 66 (A) CYS 66 (A) ALA 65 (A)	H-donor H-donor H-acceptor	3.55 3.62 3.23	-0.5 -0.5 -1.4

3.4 Study analysis of ADMET and toxicity Properties.

Table 6 shows Tromantadine under study has the molecular formula of $C_{16}H_{28}N_2O_2$ with a molecular mass of 280.41 g/mol. Tromantadine displays favorable drug-like characteristics as outlined by sundry key parameters obtained via web SwissADME.

The physicochemical properties display the molecular weight within the drug-likeness scale(<500). While The topological polar surface area (TPSA) of Tromantadine was 41.57 Å², indicating a good potential for membrane permeability**.** The value (Log P) was within a range =2, suggesting a moderate lipophilicity, which is beneficial for oral absorption. The number of rotatable bonds was seven, indicating a moderate molecular flexibility**.**

Tromantadine is soluble in aqueous solution, so it is appropriate for oral preparations. GI absorption was high, indicating a good absorption in the gastrointestinal system. while the blood-brain barrier (BBB) demonstrates a permeant ability to cross the BBB, which is useful in medications that target the CNS. Table 6 shows there is no inhibition to CYP1A2, CYP2C19, CYP2C9, CYP2D6, CYP3A4 which suggests low potential for drug-drug interactions involving these metabolic enzymes**.** The drug-likeness and medicinal chemistry results indicated a good oral bioavailability, moderate probability of oral bioavailability, and moderate ease of synthesis (from 1(easy)to 10 (difficult**)**. These findings indicate that tromantadine has a promising oral bioavailability, drug-likeness, and low toxicity potential, as well as strong gastrointestinal absorption and BBB permeability. It is not expected to inhibit key CYP450 enzymes, reducing the possibility of metabolic interactions. Its moderate water

solubility and acceptable physicochemical qualities make it a promising option for further development as an orally active medicinal drug, particularly for CNS indications due to BBB permeability (see Figure 6).

Table 6 . Predicted absorption and distribution parameters of Tromantadine

Physicochemical Properties							
Formula	**Mwt (g/mol)**	**TPAS Å²**	**HBA**	**HBD**	**Rotatable Bonds**	**Fraction Csp³**	**Mola Refractivity**
$C_{16}H_{28}N_2O_2$	280.4	41.57	3	1	7	0.25	79.70
Lipophilicity		**Water Solubility**					
Log Po/w =2.02		Log $S_{(ESOL)}$= -2.46	Soluble	Solubility9.62e-01 mg/ml		Soluble	Log $S_{(SILICOS-IT)}$ -3.01
Pharmacokinetics							
GI absorption	BBB	P-gp	CYP1A2	CYP2C19	CYP2C9	CYP2D6	Log Kp
Yes	Yes	No	No	No	No	No	-6.49 cm/s
Druglikeness						Medicinal Chemistry	
Lipinski	Ghose	Veber	Egan	Muegge	Bioavailability Score	Synthetic accessibility	
Yes	Yes	Yes	Yes	Yes	0.55	4.48	

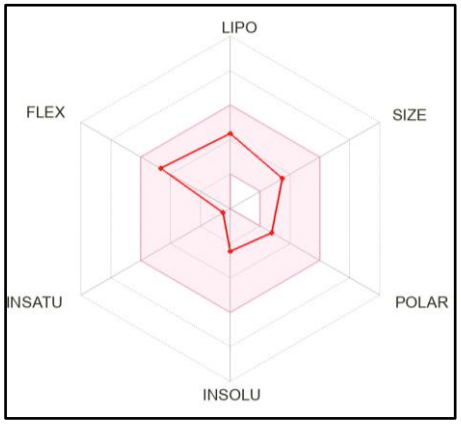


Figure 6. A spider shape of Tromantadine.

The toxicity of Tromantadine was determined using ProTox-II (website). It was expected to be non-toxic based on organ toxicity (hepatotoxicity). The toxicity-endpoint results indicated that the compound was expected to be non-mutagenic, non-cytotoxic, and non-carcinogenic. The toxicity class for the chemical was (4). Notes: Class I: lethal if eaten (LD50 ≤ 5); Class II: fatal if swallowed (5<LD50≤50). Class III is hazardous if swallowed (50< LD50≤ 300). Class IV: hazardous if swallowed (300<LD50<2000). Class V may be dangerous if eaten (LD50 <

2000), but Class VI is non-toxic (LD50>5000)[25]. The projected LD50 value suggests that the chemical is hazardous if eaten and falls into class IV (see Table 7).

Table 7. Insilco toxicity evaluation of Tromantadine.

Organ Toxicity	Toxicity - endpoints				Predicted LD50(mg/kg)	Predicted Toxicity
Hepatotoxicity	**Carcinogenicity**	**Immunotoxicity**	**Mutagenicity**	**cytotoxicity**	800	4
Inactive	inactive	inactive	Inactive	Inactive		

4. Conclusions

In this study, activity of the medicinal compound, Tromantadine, was evaluated utilizing DFT methods at B3LYP/6-31^{++}G basis. The comprehensive DFT and Fukui functions analysis of Tromantadine revealed distinct electronic features that underpin its potential biological activity. The identification of nucleophilic and electrophilic centers within the molecule, alongside a moderate HOMO-LUMO gap, indicating a balanced chemical reactivity favorable for interaction with viral targets. The calculated quantum chemical descriptors, including chemical hardness, electronegativity, softness, and electrophilicity, collectively suggest that Tromantadine possesses an electronic flexibility and polarity necessary for effective binding and interfering with viral proteins and genetic material.

These insights support the hypothesis that Teromatin could serve as a promising candidate for antiviral applications against herpes simplex virus by disrupting critical molecular interactions within the viral replication cycle. Molecular docking studies of herpes virus proteins DNA polymerase(8OJA) andGlycoprotein (3SKU) have demonstrated a complete mechanism of action, thereby confirming computational predictions of the molecule. We strongly support the need for experimental validation through laboratory-based assays based on these data.

5. Acknowledgments

The authors are thankful for the College of Science, University of Wasit for the help in doing this study.

6. Conflict of Interest

The author declares no conflict of interest. The author declares no conflict of interest.

7. References

[1] Ostheimer KE, Busch T, Görtelmeyer R, Hahn KD. Randomized double-blind trial of tromantadine versus aciclovir in recurrent herpes orofacialis. Arzneimittel-Forschung. September. 1989;39 (9):1152–1155. https://api.semanticscholar.org/CorpusID:26354703.

[2] Diezel W, Michel G, Görtelmeyer R, Ostheimer KE. Efficacy of tromantadine and aciclovir in the topical treatment of recurrent herpes orofacialis. Comparison in a clinical trial. Arzneimittel-Forschung.1993;43(4):491–496. PMID: 8494582.

[3] Rosenthal KS, Sokol MS, Ingram R L, Subramanian R, Fort RC. Tromantadine: inhibitor of early and late events in herpes simplex virus replication. Antimicrobial Agents and Chemotherapy.,December.1982;22(6):1031–1036. https://dx.doi.org/10.1128/aac.22.6.1031.

[4] Sager AG, Abaies, JK, Katoof ZR. Design, Molecular Docking, ADMET Studies, Synthesis, Characterization, and Antimicrobial of Nicotinamide Derivatives via Mannich reaction. Iraqi Journal of Science. 2025;66(3):1-17. https://dx.doi.org/10.24996/ijs.2025.66.3.2.

[5] Sager AG, Salah AS, Mekky AH. Microwave Synthesis, Characterization of Some Novel Curcumin Compound and its Metal Complexes with Antimicrobial, Antioxidant Studies. International Journal of Medical Research and Pharmaceutical. 2020;12(1):429-448.https:// doi.org/10.31838/ijpr/2020.12.01.200.

[6] Zhu XY, Li QX, Kong Y. A novel human single-domain antibody-drug conjugate targeting CEACAM5 exhibits potent in vitro and in vivo antitumor activity. Acta Pharmacologica Sinica - Natu 2024; 45(3):609-618. https://10.1038/s41401-023-01200-9.

[7] Rossmann MG. The structure of antiviral agents that inhibit uncoating when complexed with viral capsids. Antiviral Research.1989;1(1):3-13. https://10.1016/0166-3542(89)90016-8.

[8] Sundareswaran T, Jagan R, Karthikeya N, Boaz BM. Rational analysis of hydrogen bonding interaction in phenazine, 2-hydroxynaphthalene (1:1) cocrystal: from molecular modeling to photophysical properties. Ournal of Molecular Modeling. 2024;30(10): 351. https://doi.org/10.1007/s00894-024-06128-3.

[9] Bakker MJ, Mládek A, Semrád H, Zapleta V, Pavlíková Přecechtělová J. Improving IDP theoretical chemical shift accuracy and efficiency through a combined

MD/ADMA/DFT and machine learning approach. Physical Chemistry Chemical Physics. 2022;24(45):27678-27692. https://doi.org/10.1002/ardp.202400423.

[10] Prajapati P, Pandey J, Tandon P, Sinha K, Shimpi MR. Molecular structural, hydrogen bonding interactions, and chemical reactivity studies of ezetimibe-L-proline cocrystal using spectroscopic and quantum chemical approach. Frontiers in Chemistry. 2022;10:848014. https://doi.org/10.3389/fchem.2022.848014.

[11] Zayed EM, Zayed MA, Abd El Salam HA, Noamaan MA. Novel triazole thiole ligand and some of its metal chelates: synthesis, structure charactertization, thermal behavior in comparison with computational caculations and biological activities. Computational Biology and Chemistry. 2019;78:260-272. https://doi.org/10.1016/j.compbiolchem.2018.12.008.

[12] Arulaabaranam K, Muthu S, Mani G, Ben Geoffrey AS. Speculative assessment,molecular composition, PDOS, topology exploration (ELF, LOL, RDG), ligand-protein interactions, on 5-bromo-3-nitropyridine-2-carbonitrile. Heliyon. 2021; 7(5): 07061. https://doi.10.1016/j.heliyon.2021.e07061.

[13] Pinzi L, Rastelli G. Molecular docking: shifting paradigms in drug discovery. International Journal of Molecular Sciences. 2019;20(18):4331. https://doi.10.3390/ijms20184331.

[14] Morales-Bayuelo A, Sánchez-Márquez J. Receptor-based pharmacophore modelling of a series of ligands used as inhibitors of the SARS-CoV-2 virus by complementary theoretical approaches, molecular docking, an reactivity descriptors. F1000Researchs. 2023;12:749. https://doi.10.12688/f1000research.133426.1.

[15] Razooqi MS, Al-Ani HN.Quantum me chanical calculations and electrochemical study of vibrational frequencies, energies in some flavonoids molecules. Iraqi Journal Sceince. 2022;63(6):2331-2344. https://doi.10.24996/ijs.2022.63.6.2

[16] Obayes H R, Al-Amiery AA, Alwan HG, Abdullah TA, Kadhum AAH, Mohamad AB. Sulphonamides as corrosion inhibitor: experimental and DFT studies. Journal Molecular. Structure . 2017;1138:27–34. https://doi.org/10.1016/j.molstruc.2017.02.100.

[17] Stephens PJ, Devlin F, Chabalowski C, Frisch MJ. An initio calculation of vibrational absorption and circular dichroism spectra using density functional force

fields. Journal. Physical Chemical B .1994;98:11623– 11627. https://doi.org/10.1021/j100096a001.

[18] Aquino AAJ , Borges I, Nieman, R., Köhn A, Lischka H. Intermolecular interactions and charge transfer transitions in aromatic hydrocarbon-tetracyanoethylene complexes.Journals Physical Chemistry Chemical Physics. 2021;16:20586-20597.https://doi.org/10.1039/C4CP02900.

[19] Echegaray E, Cárdenas C, Rabi S, Rabi N, Lee S, Zadeh FH. In pursuit of negative fukui functions: examples where the highest occupied molecular orbital fails to dominate the chemical reactivity. Journal of Molecular Graphics and Modelling. 2019;19: 2779–2783. https://doi.10.1007/s00894-012-1637-3.

[20] Balachandar S, Dhandapani M. Biological action of molecular adduct pyrazole: trichloroacetic acid on Candida albicans and ct DNA - a combined experimental, Fukui functions calculation and molecular docking analysis. Journal of Molecular Structure. 2019; 1184:129-138. https://doi.org/10.1016/j.molstruc.2019.02.006.

[21] Parr RG, Yang W. Density functional approach to the frontier-electron theory of chemical Reactivity. Journal of the American Chemical Society. 1989;106:4049-4050. https://doi.org/10.1021/ja00326a036.

[22] Gazquez JL, Mendez F. The hard and soft acids and bases principle: an atoms in molecules Viewpoint. Journal of Physical Chemistry. 1994;984:591-4593. https://doi.org/10.1021/j100068a018.

[23] Mulliken R S. Electronic population analysis on LCAO-MO molecular wave functions.Journal of Chemical Physics. 1955;23:1833-1840. https://doi.org/10.1063/1.1740588.

[24] Laplaza R, Peccati, F, Boto RA, Quan C, Carbone A, Piquemal J-P. NCIPLOT and the analysis of noncovalent interactions using the reduced density gradient. Wiley Interdisciplinary Reviews:Computational Molecular Scienc. 2021;11(2):1-37. https://doi.org/10.1002/wcms.1497

[25] Sager A, Abbood A F, Abaies J K, Khazal F A. A design, molecular docking, ADMET studies, synthesis, characterization, and Invitro pharmacological evaluation of tetrazole derivatives. Iraqi Journal of Pharmaceutical Sciences.2025;34:10-25. https://doi.org/10.31351/vol34iss1pp10-25.